Available online at www.sciencedirect.com

ScienceDirect

Journal of Magnesium and Alloys 9 (2021) 41–56

www.elsevier.com/locate/jma

Review

Towards developing Mg alloys with simultaneously improved strength and corrosion resistance via RE alloying

Jinshu Xie[a], Jinghuai Zhang[a,*], Zihao You[a], Shujuan Liu[b], Kai Guan[c], Ruizhi Wu[a,*], Jun Wang[d], Jing Feng[a]

[a] *Key Laboratory of Superlight Material and Surface Technology, Ministry of Education, College of Material Science and Chemical Engineering, Harbin Engineering University, Harbin 150001, China*

[b] *Department of Materials Physics and Chemistry, Harbin Institute of Technology, Harbin 150001, China*

[c] *Department of Materials Science and Engineering, University of Tokyo, Tokyo, Japan*

[d] *Ningbo Branch, Ordnance Science Institute of China, Ningbo 315103, China*

Received 15 January 2020; received in revised form 15 June 2020; accepted 4 August 2020

Available online 3 October 2020

Abstract

Magnesium (Mg) alloys have received an increasing interest in the past two decades for their tremendous application potential. The strength and corrosion resistance levels of common Mg alloys are still relativity low, and especially they are to be improved simultaneously. The addition of rare earth (RE) to Mg alloys is believed to be beneficial for both the strength and corrosion resistance, and some RE-modified traditional Mg alloys have been studied and some new RE-containing Mg alloys have been developed by now. However, further simultaneous improvements in both strength and anti-corrosion require a better understanding of the behavior and mechanism of RE in Mg alloys. In this review, the common influence mechanisms of RE on mechanical and anti-corrosion properties of Mg alloys are summarized, and the latest research progress of RE-containing Mg alloys with simultaneously improved strength and corrosion resistance are introduced. It is demonstrated that the research on high-strength and high corrosion resistant RE-containing Mg alloys is still immature, and some opinions and suggestions are put forward for the synergetic improvement of the strength and corrosion resistance of Mg alloys, so as to contribute to the further development of Mg alloys with higher performance.

Keyword: Mg alloy; Rare earth (RE); High strength; Corrosion resistance.

1. Introduction

Magnesium (Mg) alloys, as "the green engineering materials in the 21st century" [1], have become an important advanced light alloy material and been listed in the national science and technology innovation development plan in China [2,3]. Mg alloys have their own advantages, such as low density, high specific strength and damping capacity. In recent years, Mg alloys have been used in aerospace, transportation and electronic communications industries [4–9]. Generally speaking, high strength and corrosion resistance are the two important indexes to measure high-performance structural metallic materials including Mg alloys. However, traditional Mg alloys exhibit relatively low mechanical properties and poor corrosion resistance compared with other metallic materials, and especially it is difficult to obtain both good indexes in a same alloy, which has seriously hindered their wide application in engineering fields [10,11]. Therefore, improving the mechanical and anti-corrosion properties of Mg alloys simultaneously is an urgent challenge to promote the application of Mg alloys. Fortunately, a large number of researchers have devoted themselves to the study of

* Corresponding authors.

E-mail addresses: jinghuaizhang@gmail.com (J. Zhang), rzwu@hrbeu.edu.cn (R. Wu).

https://doi.org/10.1016/j.jma.2020.08.016

high performance Mg alloys in recent years, and some Mg alloys with high strength and corrosion resistance have been reported [12,13]. Clever alloying design is the primary key to improve the properties of Mg alloys. Rare earth (RE) has been found to be the very effective element in Mg alloys. In fact, as alloying or microalloying element, the RE has been widely used in steel and non-ferrous alloys [14]. In the field of Mg alloys, especially for the high strength Mg alloys or corrosion resistant Mg alloys, the positive influence of RE has been gradually recognized and mastered [15–22].

Literature research shows that most of the current studies on Mg alloys only focus on certain properties [9,15,17,19-22]. For example, some studies only report on mechanical properties [9,15,17,20], while others only focus on corrosion behaviors [19,21,22]. The comprehensive mechanical and anti-corrosion properties of specific Mg alloys cannot be obtained from these reports. In fact, some alloys are designed with only one property index in mind (such as strength), while such design may have the negative effect on others (such as corrosion) [10,11,23]. It is very necessary to consider the mechanical and anti-corrosion properties of Mg alloys simultaneously, which is important for the practical application of Mg alloy materials [12,13,24]. Therefore, here we mainly select those studies as references, which report not only the mechanical properties but also the corrosion behaviors for a same RE-containing Mg alloy. In this paper, the behavior of RE in Mg alloys and its influence on mechanical and anti-corrosion properties of Mg alloys are summarized. A series of RE-containing Mg alloys with high strength and corrosion resistance are introduced, so as to clarify the current research status, and also try to summarize some common rules. It is expected to be helpful to inspire new ideas of improving the mechanical and anti-corrosion properties synergistically for Mg alloys, and to develop advanced Mg alloy materials with higher comprehensive performance.

2. Common influence mechanism of RE on mechanical properties of Mg alloys

The RE elements are composed of 17 elements, and they can be generally divided into “light RE (named as LRE)” elements (La, Ce, Pr, Nd, Pm, Sm, Eu) and “heavy RE (named as HRE)” elements (Gd, Tb, Dy, Ho, Er, Tm, Yb, Lu, Y) except Sc, according to their slight difference of physical and chemical properties, the formation characteristics of RE minerals and their different separation processes. Generally, the influence mechanism of RE on mechanical properties of Mg alloys involves at least the following aspects.

(1) Solid solution strengthening. The solid solution formed by RE atoms can increase the strength of Mg alloys. Hume-Rothery theory indicates that the solid solubility of solutes in solvents is affected by the difference of atomic radius and electronegativity [25,26]. The atomic radius and electronegativity of most RE elements are shown in Fig. 1. The atomic radius and electronegativity of Mg are 0.160 nm and 1.31, respectively. The difference of atomic radius and electronegativity between HREs and Mg are relatively small compared with those between LREs and Mg (except Eu and Yb, which are rarely used in Mg alloys), resulting in the higher solid solubility of HREs in Mg. In fact, the solid solubility of HREs in Mg is higher than that of most alloying elements in Mg alloys. Theoretical calculation indicated that the Mg matrix would produce lattice distortion when RE atoms are dissolved in Mg matrix, resulting in the interaction of dislocations and RE atoms. The dislocation/RE atom interaction energy is typically composed of specific chemical core contributions and size misfit. The former is caused by the different bonding environment within the nonlinear core and stacking fault regions of the dislocations, and the latter results from the interaction of the elastic stress field of the dislocation with the volumetric strain field around the RE elements [27]. Therefore, the dislocation motion would be severely hampered by the above interactions, so as to strengthen the Mg matrix. More recently, Mo et al. [28] designed experiments to understand the solid solution strengthening in a creep resistant Mg–Gd–Ca alloy, and they found that Gd, particularly combined with Ca, has excellent solid solution enhancement, especially at high temperatures.

(2) Fine-grain strengthening. According to the Hall–Petch relationship, grain refinement is one of the important measures to improve mechanical properties of metal materials. The refinement of solidification structure of metal and alloy materials is based on the following basic principles: (a) increasing the nucleation particle in liquid phase and promoting the nucleation rate; (b) inhibiting the growth of crystal nucleus. For the solidification of RE-containing Mg alloys, RE atoms would be into the front of solid/liquid interface due to the solute redistribution effect during solidification process. Thus, this would cause the constitutional supercooling in the front edge of crystallization, and improve the supercooling degree so as to promote the nucleation of α-Mg grains. In addition, the RE-containing secondary phases with high melting point would also be formed under certain conditions, which can further prevent the growth of α-Mg grains. According to literature reports, the most commonly used grain refined RE elements in Mg alloys are Y, Ce, Nd, Er and Sc [29–35]. Tong et al. [31] found that adding 0.5–1.5 wt% Ce into AZ91 alloy could significantly refine the alloy grain, and the average grain size decreases from 30 μm to about 10 μm when the Ce content is 1.5 wt%. Wang et al. [32] studied AZ80 alloy with and without 1.0 wt% Nd, and the results showed that the grain size is refined from 448 μm to 125 μm. Zhang et al. [33] found that adding 2 wt% Er to Mg–9Zn–0.6Zr alloy could refine the grain size from 102 μm to 32 μm.

(3) Precipitation strengthening. Nano-sized precipitates derived from addition of RE play very important role for strengthening RE-containing Mg alloys, which

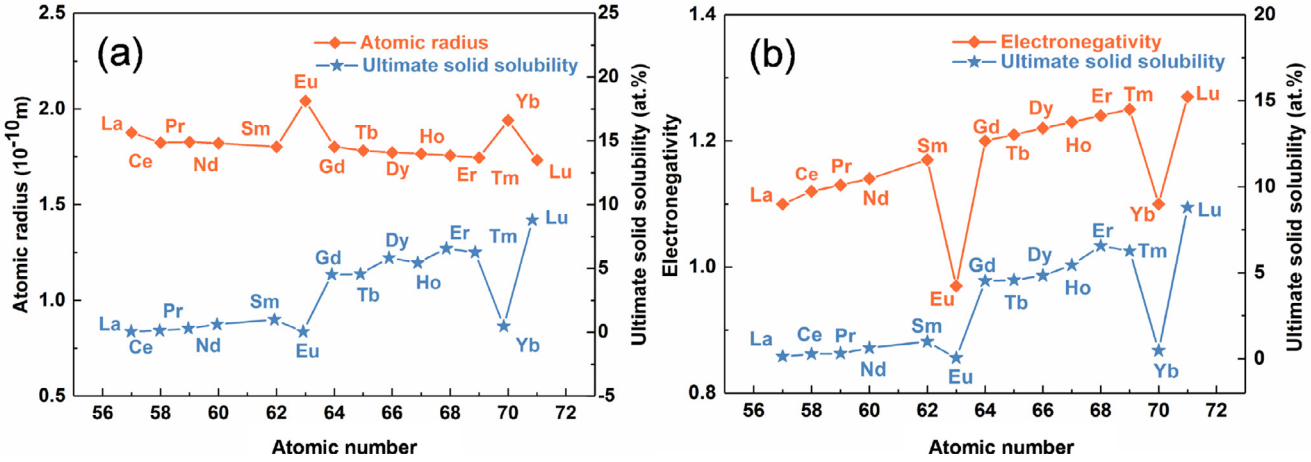

Fig. 1. (a) Atomic radius and ultimate solid solubility of RE in Mg versus RE atomic number. (b) Electronegativity and ultimate solid solubility of RE in Mg versus RE atomic number [25].

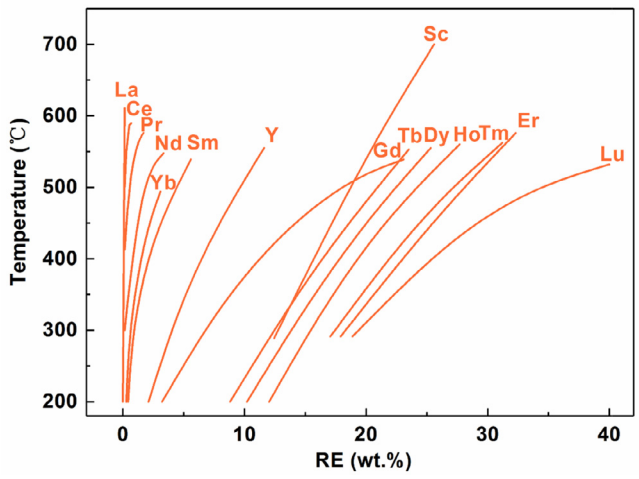

Fig. 2. Solid solubility of different REs in Mg versus temperature [25].

is a typical major strengthening mechanism for the ultra-high strength Mg alloys reported at present. As shown in Fig. 2, the solid solubility of RE elements in Mg matrix decreases with temperature dropping. When the single-phase solid solution of Mg matrix at high temperature cools down rapidly, the supersaturated solid solution would be formed. After aging treatment, numerous dispersed nano-sized precipitates could be precipitated out from the supersaturated solid solution. As for the effectiveness of precipitation strengthening, the following results can be summarized. (a) HRE-containing Mg alloys have superior aging hardening potential than LRE-containing Mg alloys (except Yb). The solid solubility of HREs in Mg matrix is much higher than that of LREs. For HREs, their solid solubility in Mg are large at high temperature and reduce greatly with the decrease of temperature, which is beneficial to improve the aging response. The most typical and common RE element for age-hardened Mg alloys is Gd. The solid solubility of Gd is 4.53 at% at the temperature of 548 °C, and only 0.35 at% at 200 °C. (b) The HREs have better effect on precipitation strengthening than other common alloying elements in Mg alloys. For example, the ultimate solid solubility of Zn in Mg is about 2.4 at%, which is much lower than HREs (except Yb) in Mg alloys. (c) Different types of RE-containing Mg alloys have different precipitation sequences as follows.

(i) Aging behavior of Mg-HRE alloys. The common precipitation sequence in Mg-HRE (Mg–Gd, Mg–Gd–Y, Mg–Gd–Nd, Mg–Y–Nd, etc.) alloys during aging process has been well recognized: SSSS→ordered G.P.zones→β''(D019)→β'(cbco)→β_1(fcc)→β(fcc) [36,37]. With the development and popularity of the high-angle annular dark-field scanning transmission electron microscopy (HAADF-STEM) technology, some new precipitated phases are found in Mg–Gd alloys, such as β'_F (Fig. 3) [38,39]. Among the precipitation sequences, the β' precipitates with nanoscale and dense distribution are generally acknowledged as the key strengthening role in peak-aged Mg–Gd(-RE) alloys, and a few reports also find that sometimes coexistence of $\beta'+\beta''$ or $\beta'+\beta_1$ is responsible for the peak aging hardening. β' precipitates have a base-centered orthorhombic structure and an orientation relationship with respect to the Mg matrix: $(100)_{\beta'}//\{1\bar{2}10\}_\alpha$ and $[001]_{\beta'}//[0001]_\alpha$ (Fig. 3). It is considered that the β' precipitates play an extremely effective role in hindering basal dislocation slip and twin propagation [37], based on the fact that they form on $\{1\bar{2}10\}$ prismatic planes of α-Mg in a dense triangular arrangement and are vertical to basal plane of α-Mg. It should also be noted that the precipitation strengthening effect is related to not only the habit plane but also the aspect ratio, number density and nanoscale.

(ii) Aging behavior of Mg-LRE alloys. The solid solubility of LREs in Mg is usually lower than that of HREs in Mg, which leads to the less number of pre-

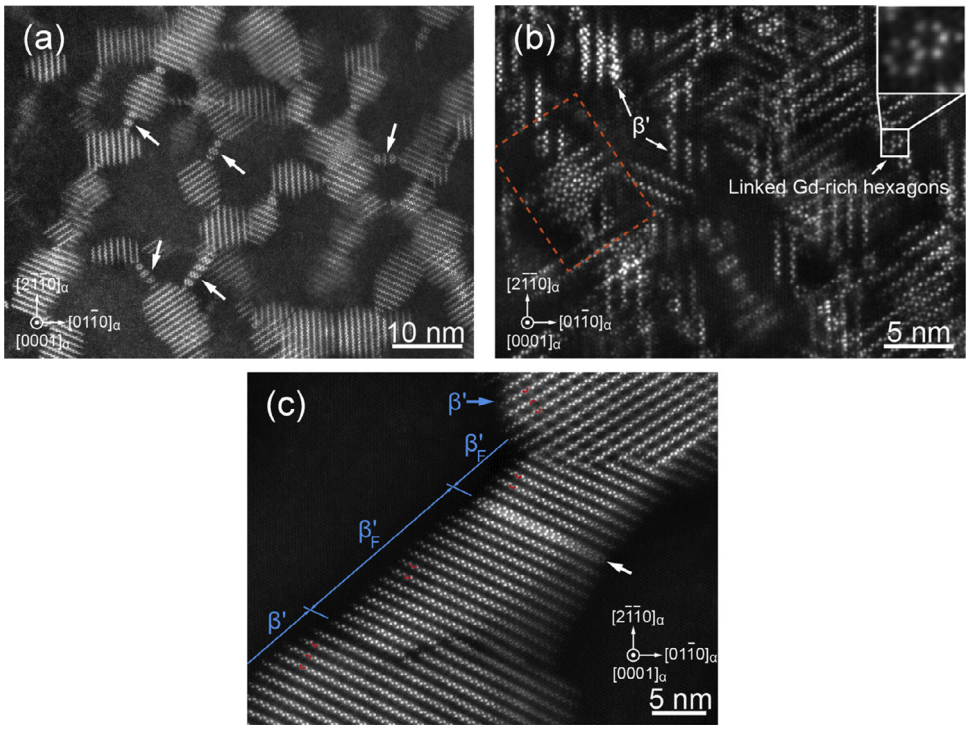

Fig. 3. HAADF-STEM images showing the morphology and distribution of β' precipitates in Mg–16.2Gd–0.4Zr (wt.%) specimens aged for (a) 128 h, (b) 2048 h and the distribution of β'_F precipitates aged at 200 °C for (c) 2048 h. Electron beam//$[0001]_\alpha$ [39].

cipitates formed during the aging process. Therefore, Mg-LRE alloys can have the aging response in the case of low content, but generally the effect of precipitation strengthening of Mg-LRE alloys is inferior to that of Mg-HRE alloys. There are less researches on the precipitation phases of Mg-LRE alloys compared with Mg-HRE alloys, and a few researches are mainly concentrated on Mg–Nd [40], Mg–Ce [41] and Mg–Sm [42] binary alloys. At present, the precipitated phases and their transition mechanism of Mg-LRE alloys have not been thoroughly studied. The current studies indicate that the precipitation phases and aging precipitation sequences are different between Mg-LRE and Mg-HRE alloys, even in different Mg-LRE alloys. Nie [37] reported that the precipitation sequence of Mg–Nd binary alloy is: S.S.S.S→ordered G.P.zones→β''(Mg_3Nd,D019)→β(Mg_7Nd,orthorhombic) → β_1(Mg_3Nd,fcc)→β($Mg_{12}Nd$,tetragonal)→β_e($Mg_{41}Nd_5$,tetragonal). In addition, Saito and Kaneki [41] found that the aging precipitation sequence of Mg-Ce binary alloy is S.S.S.S→ordered G.P.zones→β_1(Mg_3Ce,BiF_3-type)→β($Mg_{12}Ce$,$Mn_{12}Th$-type). The aging precipitation sequence of Mg-LRE alloys generally lacks the β'(cbco) phase compared with that of Mg-HRE alloys, which is the main strengthening phase of Mg-HRE alloys.

(iii) Aging behavior of Mg–HRE–Zn/Ag alloys. The precipitation phases and aging sequence of Mg-HRE alloys can be greatly changed by adding Zn and/or Ag. The addition of Zn and/or Ag to Mg-HRE alloys would promote the formation of the additional γ series precipitates on the basal plane. Nie et al. [43] proposed the whole precipitation sequence in a Mg–6Y–2Ag–1Zn–0.6Zr alloy during aging at and above 200 °C, and it is inferred to be: SSSS→G.P. zones→γ''→γ'→γ(14H-LPSO)+δ (other intermetallic particles at grain boundaries). The γ'' nano-sized phase is generally considered as a main strengthening phase in Mg-HRE-Zn/Ag alloys (Fig. 4), and it has an ordered hexagonal structure (P6/mmm, $a=0.556$ nm, $c=0.424$ nm). The orientation relationship between γ'' and α-Mg phases is $(0001)_{\gamma''}//(0001)_\alpha$ and $[10\bar{1}0]_{\gamma''}//[2\bar{1}\bar{1}0]_\alpha$. It is reported that the composition of the γ'' phase is $Mg_{70}Gd_{15}Zn_{15}$ in Mg-6Gd-1Zn-0.6Zr alloy [44]. Current studies [45,46] suggest that co-precipitation of β' prismatic precipitates and γ'' basal precipitates with the relative perpendicular relationship in Mg–HRE–Zn/Ag alloys is a more effective precipitation strengthening mechanism compared with only β' or γ'' precipitates (Fig. 5).

(4) Dispersion strengthening. The RE-containing intermetallic compounds would be formed by adding RE during the solidification of Mg alloys. Relatively speaking, LREs tend to form intermetallics more easily due to their lower solid solubility. These intermetallics generally have the common characteristics, such as high melting point and thermal stability (Table 1). Meanwhile, they are usually dispersed around the grain boundaries.

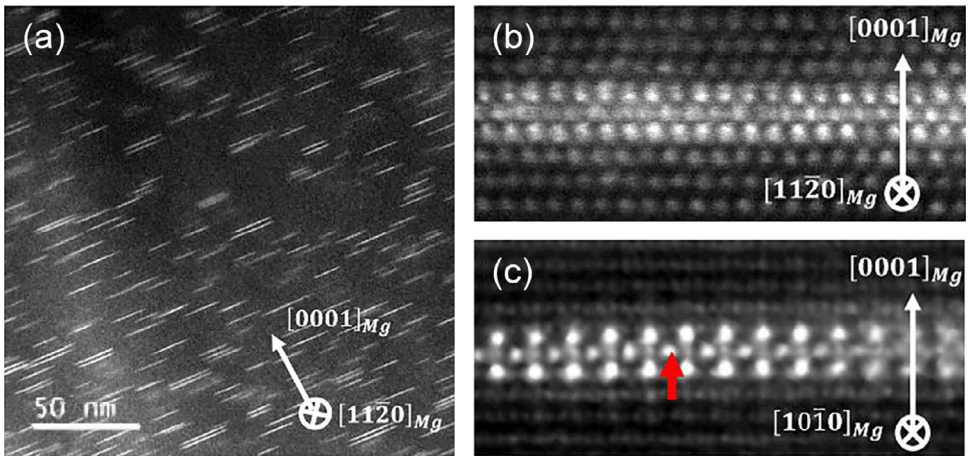

Fig. 4. (a) HAADF-STEM image of γ'' precipitates in the Mg–8Gd–4Ag–0.5Zr alloy aged at 200 °C for 3 h. Atomic-resolution HAADF images of γ'' observed from (b) $[110]_{Mg}$ and (c) $[100]_{Mg}$ [45].

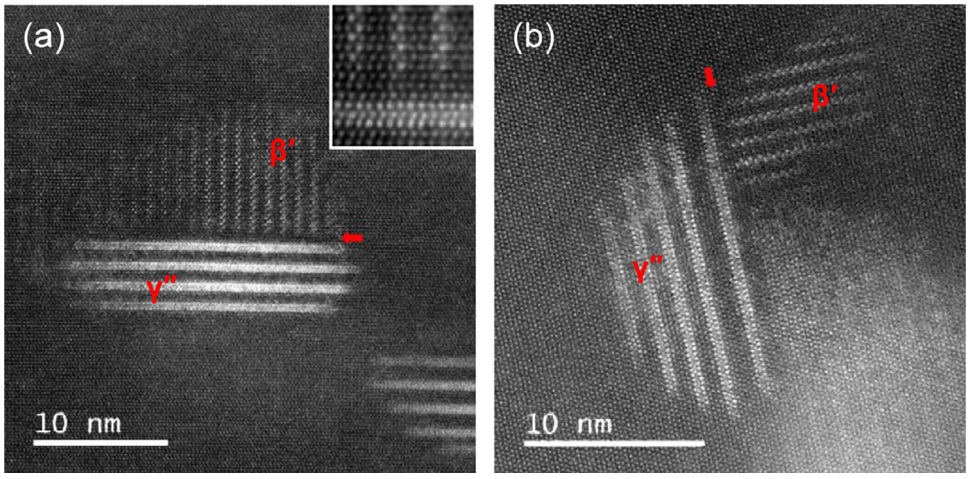

Fig. 5. HAADF-STEM images of both layered γ'' precipitates and β' precipitates in the Mg–8Gd–4Ag–0.5Zr alloy after aged at 200 °C for 32 h. Electron beam //$[11\bar{2}0]_{Mg}$ [45].

Table 1
Intermetallics and their melting point (M.P.) in Mg alloys [25].

Alloys	Phases	M.P. (°C)	Alloys	Phases	M.P. (°C)
Mg–Al	$Mg_{17}Al_{12}$	455	Mg–Yb	Mg_2Yb	718
Mg–La	$Mg_{12}La$	640	Mg–Y	$Mg_{24}Y_5$	605
Mg–Ce	$Mg_{12}Ce$	611	Mg–Al–La	$Al_{11}La_3$	1240
Mg–Nd	$Mg_{41}Nd_5$	560	Mg–Al–Ce	$Al_{11}Ce_3$	1235
Mg–Gd	Mg_5Gd	642	Mg–Al–Ce	Al_2Ce	1480
Mg–Dy	$Mg_{24}Dy_5$	610	Mg–Al–Nd	$Al_{11}Nd_3$	1235
Mg–Ho	$Mg_{24}Ho_5$	610	Mg–Al–Nd	Al_2Nd	1460
Mg–Er	$Mg_{24}Er_5$	620	Mg–Al–Y	Al_2Y	1485

Therefore, they can reinforce alloys by pinning grain boundary and hindering dislocation motion, especially at high temperature. Our team [47] and Yang et al. [48,49] devote to develop the die casting Mg–Al–RE alloys with excellent mechanical properties by controlling intermetallic phases, and we find that the densely dispersed $Al_{11}La_3$ or η-Al_3La (Fig. 6) intermetallic phases have a very effective dispersion strengthening effect.

According to the above analyses, generally speaking, the strengthening effects of solid solution and aging precipitation of HREs are superior to those of LREs, while the fine-grain and dispersion strengthening effects of LREs are better than those of HREs. Perhaps, combined additions of LREs and HREs would be a good idea to strengthen Mg alloys. Anyway, the RE-containing Mg alloys is an important research and development direction for the high-strength Mg alloy.

3. Common influence mechanism of RE on corrosion resistance of Mg alloys

The poor corrosion resistance has always been a key shortcoming of Mg alloys over the years. This is closely related to the chemical properties of Mg. Firstly, the standard electrode potential of Mg is very low (−2.37 V vs. Standard hydrogen electrode, SHE), and its chemical activity is extremely high compared with other common metals. Therefore, when Mg contact with other phase, Mg generally acts as the anode to promote micro-galvanic corrosion. The phase that becomes

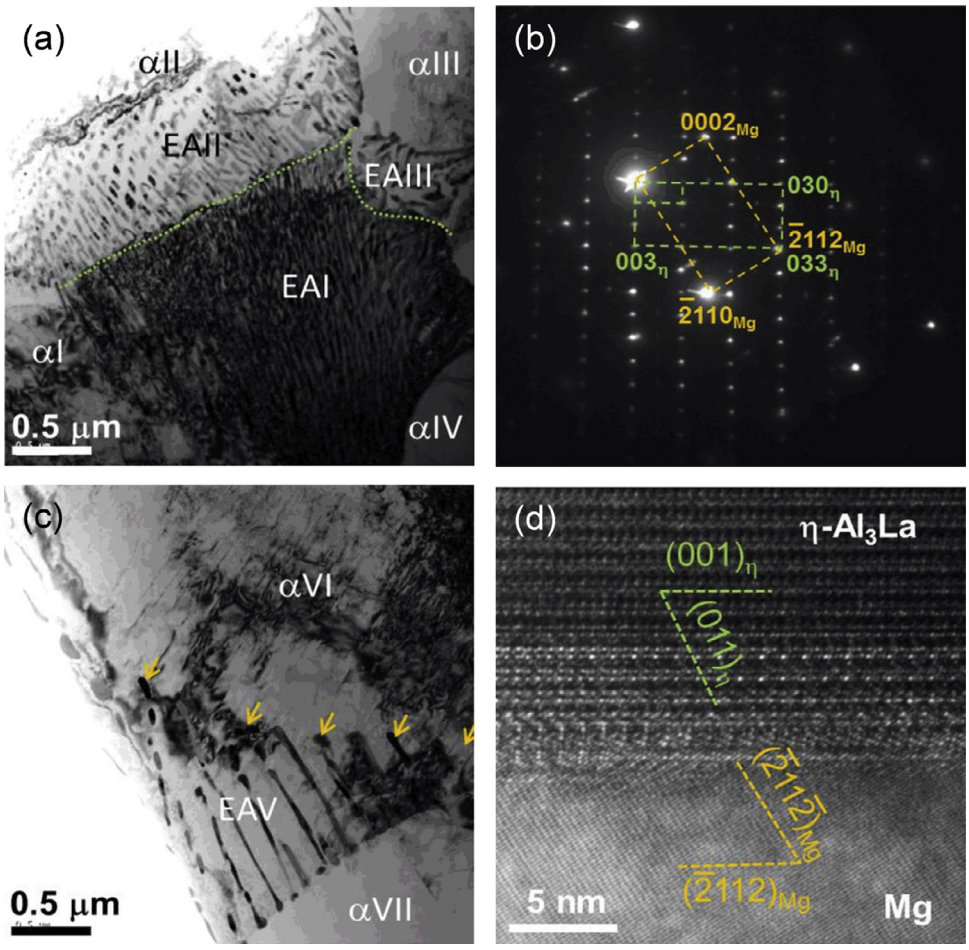

Fig. 6. (a) and (c) Bright-field transmission electron microscope (BF-TEM) images of the η-Al_3La, (b) selected area electron diffraction (SAED) pattern from a fine η-Al_3La particle and (d) the interface between η-Al_3La and Mg matrix in a Mg–Al–La die casting alloy [48].

the galvanic cathode may be other metal contacted with the Mg alloy externally, or the secondary phase or impurity inside the Mg alloy matrix [50]. Secondly, Mg is easily oxidized and forms an incomplete surface oxidation film with the value of Pilling-Bed-worth ratio (PBR) of 0.81 (<1). At the same time, the surface film (MgO) is soluble in water, and thus it can't play a long-term protective role [51]. Thirdly, there are existing "negative difference effect" in the corrosion process of Mg and its alloys, which would accelerate the evolution reaction of cathode hydrogen, resulting in that the protective film of $Mg(OH)_2$ falls off seriously and fails [52].

On pure Mg or Mg alloys, the overall corrosion reaction can be expressed as follows [53–55]:

$$Mg + 2H^+ \rightarrow Mg^{2+} + H_2 \quad \text{(in an acidic solution)}$$

$$Mg + 2H_2O \rightarrow Mg^{2+} + 2OH^- + H_2 \quad \text{(in a neutral or alkaline solution)}$$

The overall corrosion can be divided into anode and cathode reactions. The cathodic reaction is:

$$2H^+ + 2e \rightarrow H_2 \quad \text{(in an acidic solution)}$$

$$2H_2O + 2e \rightarrow H_2 + 2OH^- \quad \text{(in a neutral or alkaline solution)}$$

and the anodic reaction (y is the ratio of further anodic reaction over hydrogen production reactions):

$$Mg + [\tfrac{1}{(1+y)}]H^+ \rightarrow Mg^{2+} + [\tfrac{1}{(2+2y)}]H_2 + [\tfrac{1+2y}{(1+y)}]e \quad \text{(in an acidic solution)}$$

$$Mg + [\tfrac{1}{(1+y)}]H_2O \rightarrow Mg^{2+} + [\tfrac{1}{(1+y)}]OH^- + [\tfrac{1}{(2+2y)}]H_2 + [\tfrac{1+2y}{(1+y)}]e \quad \text{(in a neutral or alkaline solution).}$$

In view of the above problems, according to the current research status, RE alloying is an effective way to improve the anti-corrosion resistance of Mg alloys. The effect of RE alloying on the anti-corrosion properties of Mg alloys can be considered from at least the following aspects.

(1) Effect of RE on the thermodynamics of corrosion. The difference of electrode potential between common alloying elements (Al: −1.67 V, Zn: −0.76 V) and Mg (−2.37 V) is large, and the same as the formed intermetallic compounds and Mg. Therefore, the microgalvanic corrosion of common Mg alloys is serious. Compared with common alloying elements in Mg alloys, the electrode potentials of REs (Y: −2.37 V, La: −2.37 V, Gd: −2.40 V, Nd: −2.44 V, Ce: −2.48 V) are

similar to Mg, and their compounds have low electrode potentials, so as to help lower the overall potentials of the cathode phase [56]. In particular, some RE-containing secondary phases are even more positive than the Mg matrix, which is very rare in Mg alloys. For example, the electrode potentials of $Mg_{24}(Gd,Y)_5$ and $Mg_5(Gd,Y)$ are reported to be lower than that of the Mg matrix, making them as an anodic secondary phase [57,58]. Therefore, RE alloying can improve corrosion resistance of Mg alloys by reducing internal micro-galvanic corrosion. On the other hand, the "scavenging effect" is another important effect of REs on the corrosion resistance of Mg alloys. Mercer and Hill et al. [59] found that RE (Ce, La, Nd, Pr) can trap harmful elements (Fe, Ni, Cu) and form intermetallic compounds, decreasing cathode activity. Zhou et al. [60] studied the effect of adding Ho on the corrosion behavior of AZ91D and believed that the addition of Ho can reduce the concentration of Fe in the alloy, resulting in the improvement of matrix corrosion resistance.

(2) Effect of RE on the grain size. The relationship between the grain size and corrosion current density in Mg alloys (validated using ZK60) is reported to be similar to the bounds of the classical Hall–Petch relationship [61–63]. Aung and Zhou [64] found that the corrosion rates of AZ31B in 3.5 wt% NaCl solution reduces with the decrease of grain size. In addition, previous studies [65,66] about the effect of grain size on the corrosion behavior of Mg alloys have shown that grain refinement can reduce the pitting initiation by lowering the mismatch stress between Mg matrix and surface layer. Meanwhile, grain boundary is considered as a corrosion barrier to prevent corrosion progress [58]. As mentioned in the previous section, the addition of RE can effectively refine the Mg alloy grains, and studies also have shown that RE can improve the corrosion resistance of Mg alloys by grain refinement [67,68].

(3) Effect of RE on the composition, volume fraction and distribution of secondary phases. Song [69] laid the framework of the corrosion mechanism of Mg alloys by studying the influence of β-$Mg_{17}Al_{12}$ phase on corrosion behavior of Mg–Al series alloys, and also provided theoretical support for the research on the corrosion mechanism of RE-containing Mg alloys. The β-$Mg_{17}Al_{12}$ phase serves two roles, as a galvanic cathode and as a barrier. The galvanic effect is that the β-$Mg_{17}Al_{12}$ phase acts as the cathode phase of micro-galvanic corrosion to accelerate the corrosion of the matrix when the distribution is discontinuous and the volume fraction is low. Instead, the corrosion barrier effect is that the β-$Mg_{17}Al_{12}$ phase with large volume fraction and continuous distribution would act as a corrosion barrier to retard the corrosion propagation of Mg alloys to some extent (Fig. 7) [70,71]. These mechanisms have also been applied to RE-containing Mg alloys [72,73]. Liu et al. [74] showed that adding RE (Ce or La) can improve the corrosion resistance of cast AM60 alloy, and the main reason is that the addition of Ce or La changes the phase distribution and composition by reducing the content of β-$Mg_{17}Al_{12}$ phase and promoting the formation of γ-AlRE phase. Moreover, the γ-AlRE phase may have more active potential, which reduces the galvanic corrosion caused by coupling with the Mg anode phase [75]. Chang et al. [76] also found that the heat-treated Mg–Gd–Y–Zr alloy with higher RE contents has lower corrosion rate, and thus β'-Mg_7Gd precipitates in high number density and more continuous distribution are considered to act as the corrosion barrier to some extent.

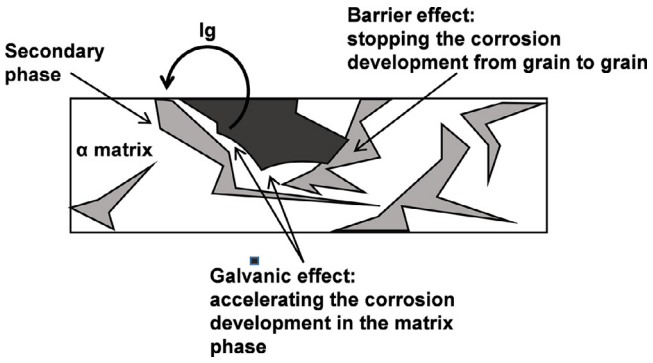

Fig. 7. Schematic illustration of the dual-role (galvanic effect and barrier effect) of the secondary phase in corrosion of Mg alloys [70].

(4) Effect of RE on the corrosion product film. The addition of RE can promote the formation of denser corrosion product films on the Mg alloys surface, so as to further improve the corrosion resistance of Mg alloys effectively [77]. It has been reported clearly that La [74], Ce [74,78], Nd [79], Er [78], Y [79,80], Gd [79,81] can increase the compactness of corrosion film of oxides or hydroxides. In addition, the PBR value [82] is usually used to represent the integrity and compactness of the oxide film. If PBR$<$1, the oxide coverage is insufficient to protect the metal; if PBR$\geq$2, the internal stress is too large, and the oxide film is easy to crack and flake; if PBR is in 1–2, a complete dense protective film can be formed. Liu et al. [79] investigated the corrosion films containing Y_2O_3, Gd_2O_3 and Nd_2O_3 of Mg–5Y–7Gd–1Nd–0.5Zr alloy, and the results showed that the PBR is in 1–2.

4. Development of high strength and corrosion resistant RE-containing Mg alloys

Despite the considerable efforts made to date, the engineering application of Mg alloys is still limited compared with that of aluminum (Al) alloys. In order to further expand the engineering application of Mg alloys, higher requirements are put forward for their strength and corrosion resistance. Fortunately, some laboratorial Mg alloys with high strength and corrosion resistance have been reported recently, and the main members are RE-containing Mg alloys. High-pressure die-cast (HPDC) Mg–Al–RE (AE) based alloys have attracted

much attention in applications of powertrain components of automobiles [83,84]. HPDC Mg–Al–Ca–RE alloys (named as ACM series by developers and ACM522 as the representative alloy) were developed specially for automobile engine oil pan by Toyota company [85]. More recently, through optimizing the composition of Mg–Zn–RE–Zr alloys, researchers found that reducing the content of Zn and increasing the RE content can improve the strength and corrosion resistance simultaneously, which could increase the feasibility of these alloys to use as transmission, valve shell, bottom shell and other parts in automobiles [86]. Furthermore, some new high performance Mg alloys with high RE content have been tried out in military fields, such as missile and aerospace components, but are less reported due to military secrecy. According to the current reports, the strength and corrosion resistance of Mg–RE, Mg–RE–Zn and Mg–Al–RE series alloys are mainly being studied.

4.1. Mg–RE alloys

The uniform corrosion behavior of as-cast Mg-10Dy alloy was found by Yang et al. [87,88], but the mechanical properties of as-cast Mg-10Dy alloy are not satisfactory. The cast Mg-10(Dy+Gd)−0.2Zr alloy was developed by partly replacing Dy with Gd in Mg-10Dy alloy, which made up for the problem that the cast Mg-10Dy alloy could not be age hardened to improve the mechanical properties [23,89]. In the as-cast condition, the alloys studied (Mg-10Dy, Mg-8Dy-2Gd-0.2Zr, Mg-5Dy-5Gd-0.2Zr, Mg-2Dy-8Gd-0.2Zr) have similar grain size (60 nm). After the solid solution treatment (T4), the grain remains the original size but the typical dendritic structure in the as-cast condition disappears. The supersaturated α-Mg solid solution is decomposed to form nano-sized β' precipitates by the subsequent aging treatment (T6). The mechanical properties of the cast Mg-10(Dy+Gd)−0.2Zr alloy can be changed over a wide range by adjusting the alloy composition and heat treatment. The ultimate tensile strength (UTS) can vary from 188 MPa to 353 MPa, yield strength (YS) can change from 99.8 MPa to 211.6 MPa, while the elongation varies from 7.8% to 24.1%. At the same time, all the cast alloys exhibit relatively uniform corrosion under solid solution state and aging condition. The Mg-2Dy-8Gd-0.2Zr alloy in aging state has the best comprehensive properties, mainly due to the more numerous nano-sized β' precipitates and more effectively protective corrosion film.

Jiang et al. [90] investigated as-cast Mg-7Y-xNd ($x=0.5$, 1.0, 1.5 wt%) alloys and the results showed that with the increase of Nd content from 0.5 to 1.5 wt%, the secondary phases would change gradually from the initial $Mg_{24}(Y,Nd)_5$ phase to the $Mg_{12}(Y,Nd)$ phase, and the UTS and YS increase from 275 MPa to 285 MPa and from 151 MPa to 165 MPa, respectively. The corrosion resistance also increases with increasing Nd content and the corrosion rate reduces from 36.75 mm/y to 19.69 mm/y in 3.5 wt% NaCl. The type and distribution of secondary phases determine that they play a dual role in the corrosion process of Mg alloys [91]. On one hand, $Mg_{24}(Y,Nd)_5$ with body-centered cubic (BCC) cell has more positive standard electrode potential than $Mg_{12}(Y,Nd)$ phase with orthorhombic cell presumably from its larger cell density leading to higher stability. Accordingly, although both secondary phases act as the cathode, the conversion of $Mg_{24}(Y,Nd)_5$ into $Mg_{12}(Y,Nd)$ reduces the micro-galvanic corrosion tendency. On the other hand, according to the corrosion barrier effect, the continuous distribution of $Mg_{12}(Y,Nd)$ along the grain boundary can retard corrosion propagation more effectively than diffusion distribution of $Mg_{24}(Y,Nd)_5$.

4.2. Mg–RE–Zn alloys

The Mg–RE–Zn alloys whose both mechanical and anti-corrosion properties have been reported include Mg–Y–Zn and Mg–Gd–Zn and Mg–Er/Ho–Zn alloys. According to the present reports, the main secondary phases vary with the mass ratio of Zn/Y [92] and Zn/Gd [93] in the former two systems. The secondary phases in Mg–Y–Zn system are I-phase (Mg_3Zn_6Y, quasicrystal structure), W-phase ($Mg_3Zn_3Y_2$, cubic structure) and X-phase ($Mg_{12}YZn/Mg_{10}YZn$, long period stacking order structure, i.e. LPSO structure) when Zn/Y are 4–6, 1.5–2 and 0.35–0.55, respectively. Similarly, these three types of secondary phases form in turn when Zn/Gd are $>$ 1.5, 1.0–1.5 and $<$ 1.0 in Mg–Gd–Zn system. Moreover, our study finds that the basal plane stacking faults (SFs) is more likely to form in the Mg–HRE–Zn alloys when Zn/HRE is very low ($\sim$0.1), especially in Mg–Er/Ho–Zn system.

4.2.1. (I+W) phases-containing Mg–HRE–Zn alloys

The I-phase has an icosahedral quasicrystal structure and fivefold symmetry axes, which possesses a quasi-lattice constant of $a_0 \approx 0.52$ nm and a valence electron concentration of $e \approx 2.1$ [94]. The I-phase can show a variety of orientation relationships with the Mg matrix. The most common one is an icosahedral twofold symmetry axis parallel to the c-axis of Mg matrix (2f$\|$[0001]), with two possible shared symmetrical variants and two other occasional variants [95–97]. In this configuration, the I-phase shows a plate-like shape on the basal plane, as shown in Fig. 8(a), and creates an interface in a low energy state. In the other configuration, the icosahedral fivefold plane matches the hexagonal plane of Mg matrix. In this type, the shape of I-phase particles is almost circular, as shown in Fig. 8(b). The I-phase with quasiperiodic crystal structure can provide very stable I-phase/α-Mg matrix interface. The W-phase possesses a partially-ordered fcc structure with $a=0.6848$ nm [98]. The morphology of the W phase is shown in Fig. 8(c). Because of the limited symmetry of the crystal lattice structure of W-phase and the incoherence of W-phase/α-Mg interface, the atomic bond between W-phase and Mg matrix is weak. In Mg-Zn-Y series alloys, the W-phase coexists with I-phase sometimes, and the interface energy of the two phases is low (Fig. 8d) [96,99].

Zhang et al. [100] comparatively studied three Mg–Zn–Y alloys with different Zn/Y mass ratios and secondary phases: Mg-1.98Zn-0.36Y (Zn/Y: 5.5, single I-phase), Mg-1.84Zn-0.82Y (Zn/Y: 2.2, both I-phase and W-phase) and Mg-1.73Zn-1.54Y (Zn/Y: 1.12, single W-phase). In the as-cast state, the

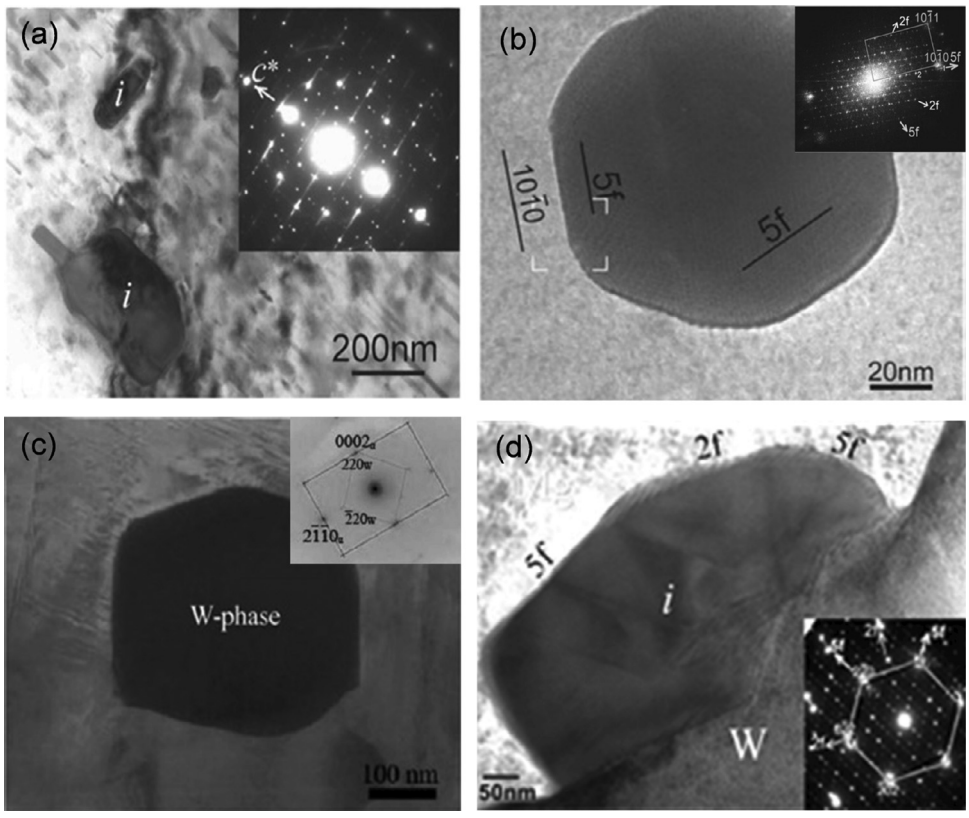

Fig. 8. (a) TEM image of plate-like I-phase particle in Mg–2.5Zn–0.5Y alloy and the corresponding composite diffraction pattern [96]; (b) TEM image of circular I-phase particle in Mg–4.2Zn–0.8Y alloy and the fast Fourier transform (FFT) pattern [96]; (c) TEM image of W-phase and its corresponding diffraction pattern in Mg–Zn–Y–Zr alloy [98]; (d) TEM image of I-phase grown on W-phase in Mg–2.5Zn–0.5Y alloy and its corresponding diffraction pattern [96].

strengthening effect of I-phase is better than that of W-phase, due to its smaller size and stronger interface. Moreover, because of the quasicrystal structure, the dislocation is entangled along it, which would be difficult to move [101]. In the as-extruded state, the I-phase can effectively inhibit the grain growth in dynamic recrystallization. Moreover, some researchers believe that both of I-phase and W-phase can promote recrystallization by regulating their morphology and size [102]. Therefore, they have a significant effect of fine-grain and dispersion strengthening. For corrosion resistance, the results showed that the extruded alloys with single I-phase as the secondary phase exhibit the lowest corrosion rate. It is worth noting that the potential difference values between the W-phase/Mg matrix and I-phase/Mg matrix are measured to be about 120 mV and 25 mV, respectively (Fig. 9) [73,103]. Therefore, although both of them can induce micro-galvanic corrosion, I-phase acts as the weaker cathodic site. Similarly, Srinivasan and Buzolin [104,105] also found the similar microstructure, mechanical and anti-corrosion mechanisms in Mg–Zn–Gd alloys as those in Mg–Zn–Y alloys.

4.2.2. LPSO phases-containing Mg–HRE–Zn alloys

In 2001, the ultra-high strength $Mg_{97}Y_2Zn_1$ (at.%) alloy was prepared by rapid solidification powder metallurgy (RSP/M), and it was found to form a special LPSO structure [106,107]. By now the LPSO structure has received extensive attention and has been introduced in Mg–RE–M (RE = *Y*, Gd, Dy, Ho, Er, Tb, Tm; *M* = Ni, Cu, Zn or Co) system, and Mg–RE–Zn alloys are the most potential and widely studied system. LPSO structure is not only stacking ordered but also chemically ordered structure, and the Mg positions on neighboring {0001} planes are occupied by RE and Zn atoms. They share the {0001} basal plane of Mg but are stacking ordered along the c-axis, resulting in stacking periods such as 10H, 14H, 12R, 18R and 24R. However, the detail structure, including the positions of Zn and RE atoms, remains controversial [108–112]. In generally, Mg–Y–Zn and Mg–Gd–Zn series are the most popular alloys containing LPSO structure, and 18R-LPSO and 14H-LPSO structures are the most common. Nie et al. [108–110] studied the structure of LPSO in Mg–Y–Zn alloy. The 18R-LPSO is an ordered base-center monoclinal structure ($a = 1.112$ nm, $b = 1.926$ nm, $c = 4.689$ nm, $\beta = 83.25°$) and composed of $Mg_{10}Y_1Zn_1$. The stacking sequence of the closely packed planes is ABABCACACABCBCBCABA, and the orientation relationship between 18R-LPSO phase and α-Mg matrix is $(001)_{18R}//(0001)_\alpha$ and $[010]_{18R}//\langle 1\bar{2}10\rangle_\alpha$ (Fig. 10). The 14H-LPSO structure is an ordered hexagonal structure ($a = 1.112$ nm, $c = 3.647$ nm) and composed of $Mg_{12}Y_1Zn_1$. The stacking order of the closely packed planes is ABABCACACACBABA, and the orientation relationship between 14H-LPSO and α-Mg matrix is $(0001)_{14H}//(0001)_\alpha$ and $\langle 0\bar{1}10\rangle_{14H}//\langle 1\bar{2}10\rangle_\alpha$ (Fig. 11).

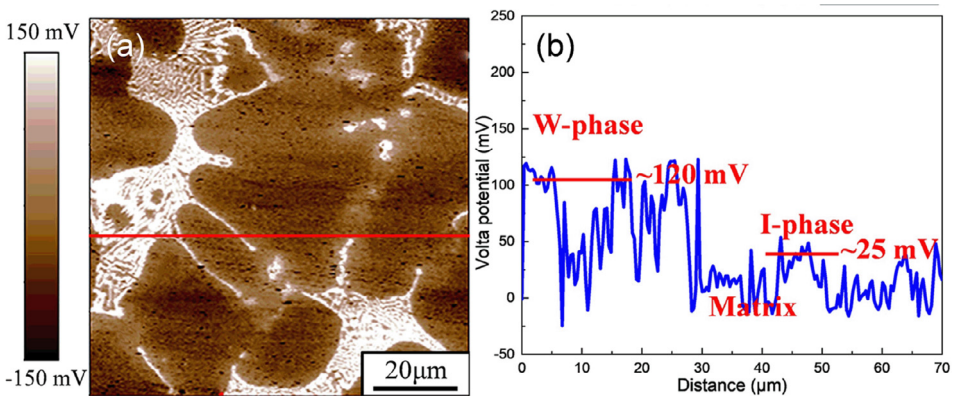

Fig. 9. Scanning Kelvin probe force microscopy (SKPFM) result of as-cast Mg–6.87Zn–4.91Gd–0.42 Zr alloy: (a) surface voltage potential map and (b) corresponding line-profile analysis of relative potential through the secondary phases [73].

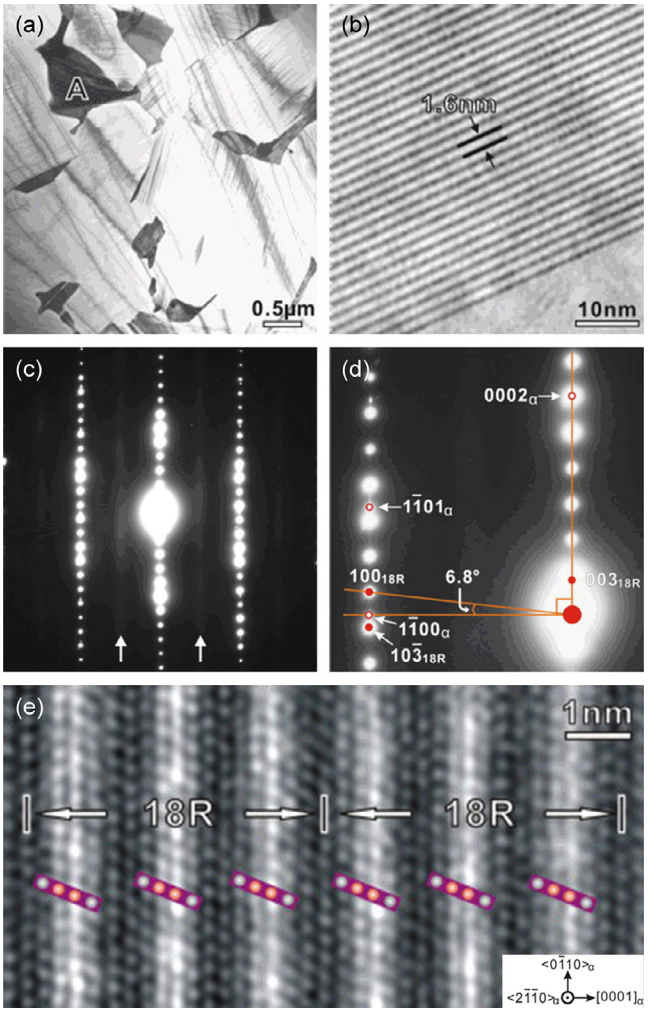

Fig. 10. (a) BF-TEM image showing particles at grain boundaries and fine precipitate plates inside α-Mg grains in as-cast Mg–8Y–2Zn–0.6Zr alloy; (b) enlargement of a local region of particle A in (a) showing the characteristic feature of 18R-LPSO; (c,d) SAED patterns of 18R-LPSO; (e) Fourier-filtered HAADF-STEM image of 18R-LPSO [108,110].

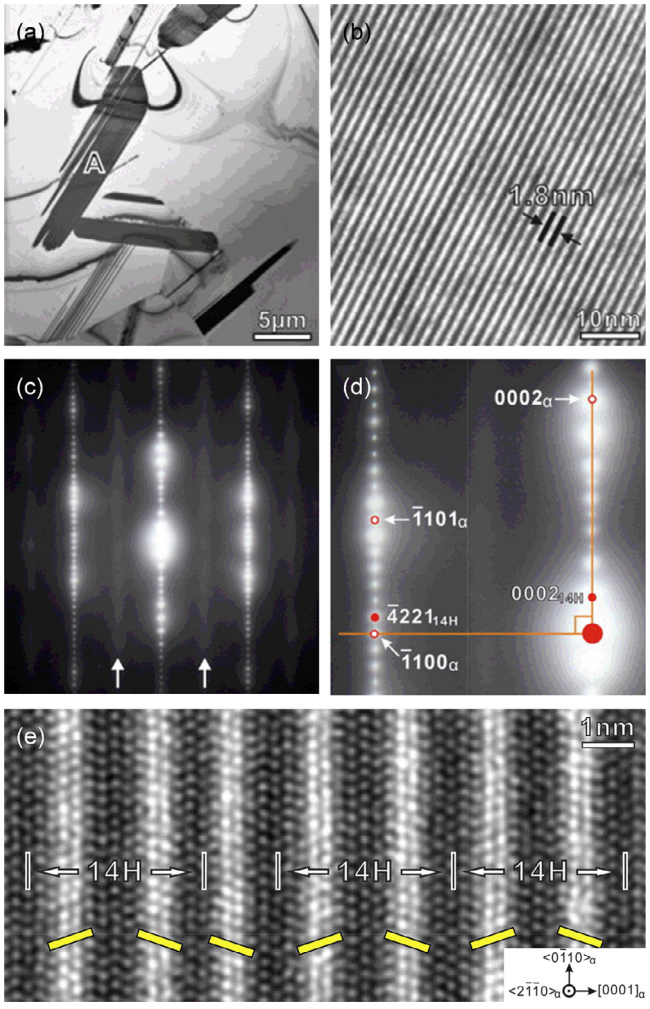

Fig. 11. (a) BF-TEM image showing particles at the grain boundaries in Mg–8Y–2Zn–0.6Zr alloy after heat-treatment at 500 °C for 60 h; (b) enlargement of a local region of particle A in (a) showing the characteristic feature of 14H-LPSO; (c,d) SAED patterns of 14H-LPSO; (e) Fourier-filtered HAADF-STEM image of 14H-LPSO [108,110].

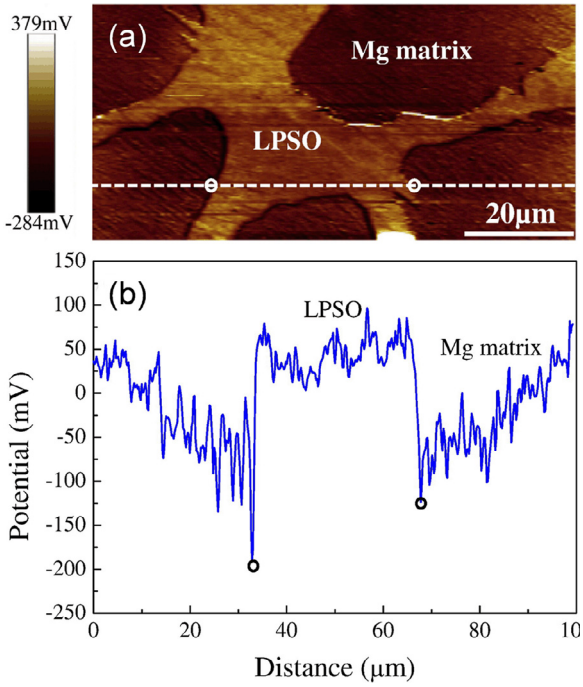

Fig. 12. SKPFM result of as-cast Mg–7.6Y–3.1 Zn alloy: (a) surface voltage potential map and (b) corresponding line-profile analysis of relative potential through the secondary phase [113].

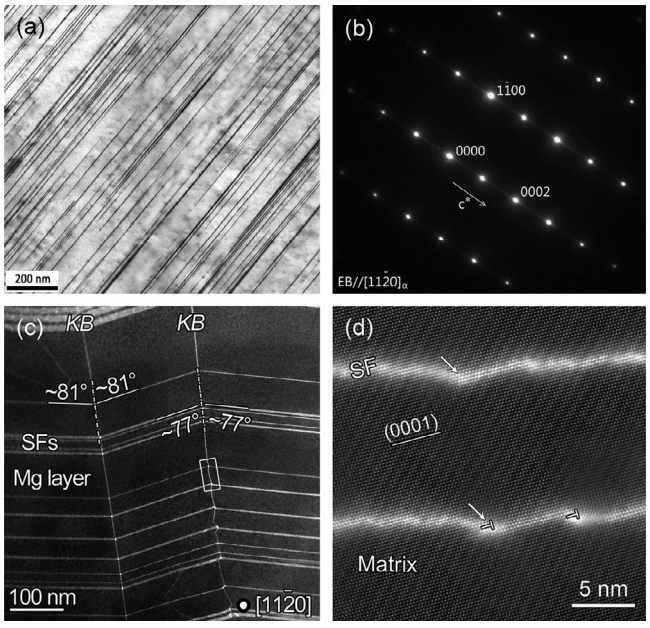

Fig. 13. (a) BF-TEM image showing the morphology of SFs and (b) SAED pattern of Mg matrix with SFs [122]; (c, d) HAADF-STEM images showing the deformation kink of SFs [118].

The stability of the 14H-LPSO phase is higher than that of the 18R-LPSO phase. After proper heat treatment, the 18R-LPSO structure can be replaced by the 14H-LPSO structure.

In recent years, numerous studies have been conducted on the microstructures, mechanical and anti-corrosion properties of Mg alloys with different LPSO structures [113–117]. Xu et al. [113] studied the microstructure evolution, anti-corrosion and mechanical properties of Mg-1.6Y-0.9 Zn (WZ21, wt%), Mg-5.2Y-2.1 Zn (WZ52) and Mg-7.6Y-3.1 Zn (WZ83) cast alloys with the different volume fractions (3.6%, 20.3% and 36.2%) of 18R-LPSO phase. The potential difference at the LPSO/α-Mg interface was measured to be 250 mV by SKPFM, indicating that LPSO phase acts as micro-cathode to accelerate the corrosion process (Fig. 12). As a result, WZ21 cast alloy exhibits the best corrosion resistance (1.05 mm/y in 0.1 M NaCl) because of the least volume fraction of LPSO phase. However, WZ83 cast alloy with the largest volume fraction of LPSO phase does not exhibit the worst corrosion resistance, which is attributed to the denser and continuous LPSO phase hindering the corrosion progress to a small degree. LPSO phase is confirmed to increase the mechanical strength of cast Mg–Zn–Y alloys when its volume fraction is below 20.3%, but overall the mechanical strength of these alloys with coarse LPSO phase in as-cast state is relatively low (< 150 MPa). Zhang et al. [114] designed Mg–Y–Zn–Zr alloys with LPSO phase and studied the influence of hot extrusion on microstructure, mechanical and anti-corrosion properties. Deformation processing such as hot extrusion is a very effective method for refining the LPSO phase and making it uniform dispersion, thus greatly improving its positive effects on mechanical and anti-corrosion properties. The results showed that the as-extruded $MgY_{3.8}Zn_3Zr_{0.18}$ (at%) alloy owns the maximum UTS and YS of 420 MPa and 300 MPa, respectively, as well as the excellent corrosion resistance. Zhang et al. [115] studied the extruded Mg-8Y-1Er-2 Zn (wt%) alloy and the results indicated that its tensile properties still remain at a high level (YS: 216 MPa, UTS: 286 MPa, elongation: 6.8%) after corrosion for 10 days, owing to formation of 18R-LPSO phase. More importantly, Peng and Liu et al. [116,117] demonstrated that the fine 14H-LPSO lamellae with uniform dispersion within grains can improve the electrochemical uniformity and reduce micro-galvanic corrosion and meanwhile, they can promote a homogeneous oxidation film with rapid film remediation ability to improve the local breakdown resistance of the film.

4.2.3. SFs-containing Mg–HRE–Zn alloys

Basal plane SFs in Mg–HRE–Zn alloys are thoroughly documented to be enriched with Zn/Y atoms and contain AB'C'A building block, similar to the LPSO phase [118]. They have more uniform distribution and finer morphology compared with LPSO phase, and their deformation kink is one of the major deformation mechanisms and responsible for the high strength and ductility (Fig. 13). Previous studies usually found a few SFs or SFs+LPSO structure in Mg–RE–Zn alloys [119–121]. More recently, our team [30,122–124] have achieved the formation of profuse nano-spaced SFs in Mg matrix almost without other secondary phases, and prepared a series of new Mg–HRE–Zn alloys via clever design of composition and preparation process.

A new Mg–8Er–1Zn extruded alloy with outstanding overall performances has been developed and deeply studied

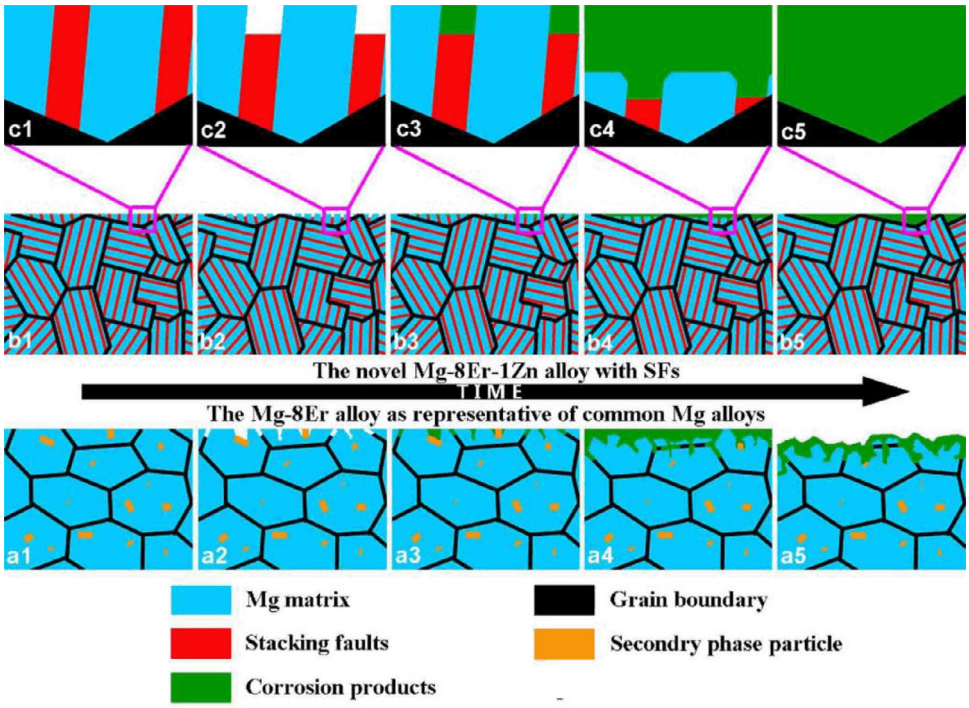

Fig. 14. Schematic diagrams of morphology during corrosion process to compare the Mg–8Er–1Zn alloy with SFs and Mg–8Er alloy with common secondary phase. a1-a5 graphs correspond to the Mg–8Er alloy; b1-b5 graphs correspond to the new Mg–8Er–1Zn alloy with profuse SFs; c1-c5 graphs represent the local amplification of b1-b5 [122].

[122]. Benefiting from the formation of profuse nano-spaced solute-segregated basal plane SFs, the alloy exhibited high strength (YS: 207 MPa, UTS: 318 MPa), high ductility (elongation: 21%), and uniquely uniform corrosion mode. Two SFs related mechanisms contribute to the excellent mechanical properties: (a) the blocking of dislocations by SFs and the cutting of SFs by dislocations would increase the strength effectively; (b) SFs can accumulate dislocations, enhance strain hardening and contribute to retaining ductility [125]. We proposed an original uniform corrosion mechanism for the novel Mg alloy with SFs for the first time based on the characteristics of SFs, i.e. segregated/defect structure, nanoscale, special orientation/distribution and promoting quickly effective film formation (Fig. 14). Therefore, this SFs-strengthened Mg alloy would be a potential engineering material with highly desirable performances.

4.3. Mg–Al–RE alloys

The Mg–Al–RE alloys are developed for engineering application and are mainly divided into two types: new developed Mg–Al–RE series and RE-modified commercial AZ series. Most of them are prepared by HPDC process. Here, these two series alloys are discussed separately, and then the strength and corrosion resistance reported by now for Mg–Al–RE alloys are evaluated by comprehensive comparison.

New Mg–Al–RE (RE=Ce-rich misch metal) series are first developed by Norsk Hydro ASA [126,127], in which AE44 alloy exhibits better mechanical property, creep resistance and corrosion resistance, and is used to fabricate automotive parts such as engine cradle for Corvette Z06 car. Since then, the famous AE44 alloy has been acted as the benchmark alloy for the development of new high-performance HPDC Mg alloys. Zhang et al. [128–131] further developed the HPDC Mg–4Al–4RE–0.4Mn (RE = La, Ce/La mixed RE, Ce, Pr or Nd) alloys and studied their microstructures, mechanical and anti-corrosion properties. The results showed that addition of RE to Mg–4Al–0.4Mn alloy leads to the complete suppression of β-$Mg_{17}Al_{12}$ phase and formation of $Al_{11}RE_3$ and Al_2RE strengthening phases, while the content, proportion, morphology and stability of the Al–RE phases are different in different Mg–Al–RE alloys. The significantly improved tensile strength is mainly attributed to the grain refinement and formation of numerous Al–RE intermetallics caused by the addition of RE. The corrosion potential of newly formed AlRE phase (γ phase) is lower than that of β-$Mg_{17}Al_{12}$ phase, making it act as the weaker cathode phase in the process of galvanic corrosion and thus improving the corrosion resistance of Mg–4Al–4RE alloys.

Liu and Niu et al. [75,132] studied the AZ91 cast Mg alloy with addition of RE (Ce/La mixed RE, 1 wt%), and the results indicated that the potentials of α-Mg, β-$Mg_{17}Al_{12}$ and γ-AlRE phases are −1.66 V, −1.20 V and −1.44 V (vs. SCE), respectively. The potential difference between α and β phases is 460 mV, while that of α and γ phases is only 220 mV (less than half of the former), and consequently the micro-galvanic corrosion effect of AZ91 alloy is greatly weakened due to addition of RE. In addition, the formed lamellar eutectic structure near grain boundaries acting as a corrosion barrier to some extent and the formation of denser corrosion product

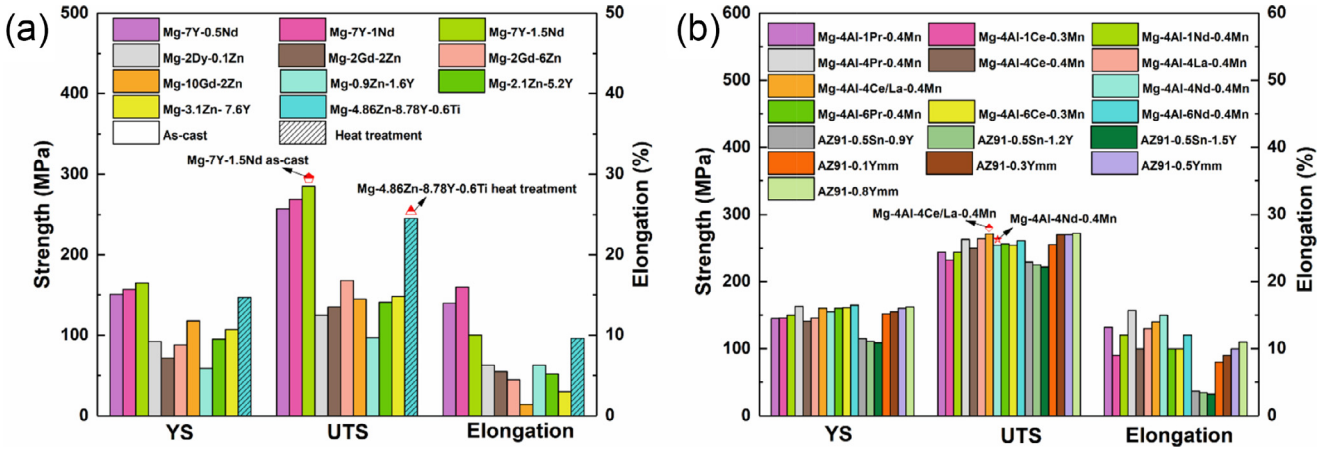

Fig. 15. Mechanical properties of the engineering (a) Mg–RE(-Zn) alloys and (b) Mg–Al–RE alloys [90,104,113,114,128–131,133–136].

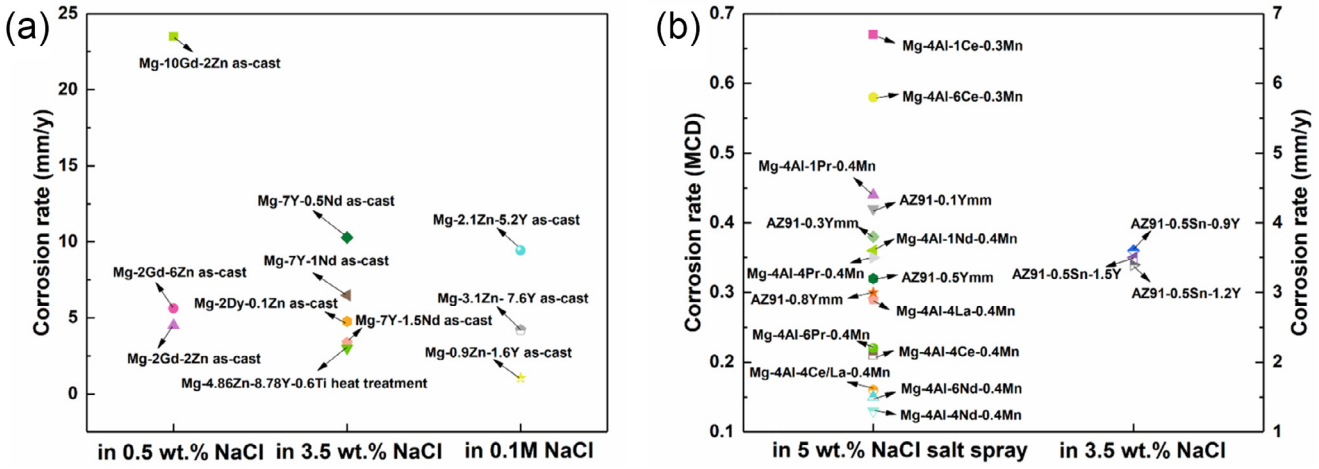

Fig. 16. Corrosion rates of the corresponding engineering (a) Mg–RE(-Zn) alloys and (b) Mg–Al–RE alloys in Fig. 15 [90,104,113,114,128-131,133–136].

film containing RE, also contribute to the improved corrosion resistance of AZ91–1RE alloy. Zhang et al. [133] found that adding a small amount of Y-rich misch metal (Ymm) in HPDC AZ91 alloy can dramatically refine both the primary α-Mg grains and β-$Mg_{17}Al_{12}$ particles. The refinement of microstructure results in the increase of the strength and plasticity synergistically. The UTS, YS and elongation of AZ91–0.8Ymm are 270 MPa, 160 MPa and 11%, respectively. The decrease of area ratio of β-$Mg_{17}Al_{12}$ phase to adjacent α-Mg grain due to the refining effect of Ymm, leads to the decline of micro-galvanic corrosion. When the content of Ymm is above 0.3 wt%, the salt-spray corrosion resistance of AZ91-Ymm alloys is 30–40 times larger than that of AZ91.

4.4. Comprehensive comparison about strength and corrosion resistance of RE-containing Mg alloys

Fig. 15 presents the mechanical properties of RE-containing Mg alloys, and Fig. 16 shows the anti-corrosion properties of the corresponding alloys in Fig. 15 reported by now. Noted that those Mg–RE(-Zn) alloys are in as-cast or cast+heat treated states and Mg–Al–RE alloys are in HPDC state, indicating lack of data of deformed RE-containing Mg alloys. It can be derived from Fig. 15(a), Mg–RE(-Zn) alloys exhibit a large range of UTS (from 97 MPa to 285 MPa), YS (from 59 MPa to 165 MPa) and elongation (from 1.4% to 16%). As shown in Fig. 15(b), Mg–Al–RE alloys exhibit a small variation range of UTS (from 222 MPa to 272 MPa), YS (from 109 MPa to 165 MPa) and elongation (from 3.2% to 15.7%). As illustrated in Fig. 16(a), the corrosion rates of Mg–RE(-Zn) alloys range from 4.51 mm/y to 23.5 mm/y in 0.5 wt% NaCl, from 3 mm/y to 10.29 mm/y in 3.5 wt% NaCl and from 1.05 mm/y to 9.44 mm/y in 0.1 M NaCl. It can be seen from Fig. 16(b), the corrosion rates of HPDC Mg–Al–RE alloys range from 0.13 mg/cm^2/day (MCD) to 0.67 MCD in 5 wt% NaCl salt spray, and from 0.34 mm/y to 0.36 mm/y in 3.5 wt% NaCl. From the comprehensive view of mechanical and anti-corrosion properties, the as-cast Mg-7Y-1.5Nd alloy (UTS: 285 MPa, YS: 165 MPa, elongation: 10%, corrosion rate: 3.37 mm/y) and the LPSO-strengthened Mg-9Y-5Zn-0.6Ti cast alloy (UTS: 245 MPa, YS: 147 MPa, elongation: 9.6%, corrosion rate: 3 mm/y) present the relatively better comprehensive performance in the developed engineering Mg alloys. Note that since these data of LPSO phase-containing Mg–RE(-Zn) alloys are from as-cast alloys, and the size of LPSO phase is relatively large, it can be

inferred that the strength and corrosion resistance of the microstructure can be further improved simultaneously after deformation processing along with the microstructure refinement. Moreover, the HPDC Mg–4Al–4Nd–0.4Mn alloy (UTS: 254 MPa, YS: 155 MPa, elongation: 15%, corrosion rate: 0.13 MCD) has excellent performance, while if the cost is also taken into account, the HPDC Mg–4Al–4Ce/La–0.4Mn alloy (UTS: 271 MPa, YS: 150 MPa, elongation: 14%, corrosion rate: 0.16 MCD) has more application potential in fields such as automobiles, due to the much lower price of Ce/La misch metal.

5. Conclusion and future trends

5.1. Summary

We have systematically summarized the main strengthening and corrosion resistant mechanisms of RE in Mg alloys, and then introduced the latest research progress of high-strength and corrosion resistant RE-containing Mg alloys. According to the current reports on studying both the mechanical and anti-corrosion properties of RE-containing Mg alloys, we inspire new ideas of improving the mechanical and anti-corrosion properties synergistically for Mg alloys.

The core problem for the mismatch of strength and corrosion resistance of Mg alloys is the non-uniformity of microstructure, that is, the difference of local composition and structure leads to the different potential. Therefore, forming the microstructure as uniform as possible and having adequate strengthening mechanism simultaneously is the key to achieve both high strength and corrosion resistance for Mg alloys. Current studies try to obtain the uniform microstructure from the aspects of refining the matrix grains and regulating the type, size and distribution of the reinforcing phase/structure. The effect of RE on grain refinement of Mg alloys is generally recognized to improve both strength and corrosion resistance. From the perspective of regulating the reinforcing phase/structure in RE-containing Mg alloys, the following main conclusions can be drawn.

(1) For the nano-sized precipitates, such as β' and γ'', they have been recognized as the extremely effective strengthening source. On the other hand, the dispersion and nanoscale of precipitates can realize the microstructure uniformity to a certain extent, and help to form smaller cathode–anode couple, resulting in lower local micro-galvanic corrosion.
(2) For the various intermetallic compounds formed during the solidification of alloys, their strengthening effect are influenced by the type, size and distribution. No matter what kind of intermetallics, only when their size is relatively small and distribution is relatively uniform, they can strengthen the alloy more effectively. In terms of corrosion behavior, size and distribution of intermetallics are also important factors, besides the difference of their electrode potential. The formation of a continuous distribution of intermetallics around grain boundaries, causing the corrosion barrier effect, can retard the spread of corrosion, while the strong galvanic corrosion always exists, and thus this state is not the fundamental and most effective way to prevent corrosion.
(3) In RE-containing Mg alloys, the quasicrystal and LPSO compounds are more concerned due to the special structures, and are considered to have great potential to improve strength. For the special LPSO phase, the fine 14H-LPSO lamellae with uniform dispersion within grains can improve the electrochemical uniformity and reduce micro-galvanic corrosion and meanwhile, they can promote a homogeneous oxidation film with rapid film remediation ability to improve the local breakdown resistance of the film.
(4) As the newly developed SFs-enhanced Mg–RE–Zn alloys, the uniform microstructure based on high-number density basal plane SFs can be constructed through clever composition and process design, so as to realize the high feasibility of simultaneously improving the high strength and corrosion resistance.

5.2. Outlook and challenges

The development of RE-containing Mg alloys is a complex process, and has been extensively studied for decades. However, there are few studies and reports on improving strength and corrosion resistance synergistically by now. Based on this review, we highlight some existing issues and challenges in this field, and outlook the work that remains open.

(1) The strength and corrosion resistance of deformed RE-containing Mg alloys based on engineering applications are rarely reported simultaneously thus far, and therefore, the intensive research in this field is necessary in the future.
(2) The experimental conditions usually are not unified, and it is difficult to conduct a uniform performance evaluation, especially in terms of corrosion.
(3) The application background of developed Mg alloys is generally not specific. The related research is not mature and far from practical application.
(4) The relevant synergistic improvement law and mechanism of strength and corrosion resistance is not yet clear. From the perspective of the reinforcing phases in RE-containing Mg alloys, it is necessary to regulate their morphology and distribution to obtain better comprehensive performance of strength and corrosion resistance based on clearly knowing their influence law and mechanism on strength and corrosion resistance.
(5) In view of the strategic value of RE resources, the development of RE-containing Mg alloys should consider how to achieve high strength and corrosion resistance on the basis of low RE content without wasting precious RE resources.

Declaration of Competing Interest

The authors declare that they have no known competing financial interests or personal relationships that could have appeared to influence the work reported in this paper.

Acknowledgments

This work was supported by National Natural Science Foundation of China (51871069), Domain Foundation of Equipment Advance Research of 13th Five-year Plan (61409220118) and Science and technology innovation major project of Ningbo City (2019B10103).

References

[1] C.X. Shi, H.D. Li, D.Z. Wang, T.Y. Zuo, Y.Y. Li, Mater. Rep. 15 (2001) 5–6.
[2] J.F. Song, J. She, D.L. Chen, F.S. Pan, J. Magn. Alloy 8 (2020) 1–41.
[3] X.J. Wang, D.K. Xu, R.Z. Wu, X.B. Chen, Q.M. Peng, L. Jin, Y.C. Xin, Z.Q. Zhang, Y. Liu, X.H. Chen, G. Chen, K.K. Deng, H.Y. Wang, J. Mater. Sci. Technol. 34 (2018) 245–247.
[4] Q. Luo, Y.L. Guo, B. Liu, Y.J. Feng, J.Y. Zhang, Q. Li, K. Chou, J. Mater. Sci. Technol. 44 (2020) 171–190.
[5] T.M. Pollock, Science 328 (2010) 986–987.
[6] M. Duan, L. Luo, Y. Liu, J. Alloy. Compd. 823 (2020) 153691.
[7] T.T.T. Trang, J.H. Zhang, J.H. Kim, A. Zargaran, J.H. Hwang, Nat. Commun. 9 (2018) 2522.
[8] Q.M. Peng, Y. Sun, J. Wang, Q. Zu, M. Yang, H. Fu, Acta Mater. 192 (2020) 60–66.
[9] S.H. You, Y.D. Huang, K.U. Kainer, N. Hort, J. Magn. Alloy 5 (2017) 239–253.
[10] L.Y. Chen, J.Q. Xu, H. Choi, M. Pozuelo, X. Ma, S. Bhowmick, J.M. Yang, S. Mathaudhu, X.C. Li, Nature 528 (2015) 539–543.
[11] Y.W. Song, E.H. Han, D.Y. Shan, C.D. Yim, B.S. You, Corros. Sci. 60 (2012) 238–245.
[12] G.Y. Yuan, X.B. Zhang, J.L. Niu, H.R. Tao, D.Y. Chen, Y.H. He, Y. Jiang, W.J. Ding, Chin. J. Nonferrous Met. 21 (2011) 2476–2488.
[13] D.K. Xu, E.H. Han, Y.B. Xu, Prog. Nat. Sci. 26 (2016) 117–128.
[14] Y. Wang, Z. Zhang, R.Z. Wu, J.F. Sun, Y.L. Jiao, L.G. Hou, X.L. Li, J.H. Zhang, M.L. Zhang, Mater. Sci. Eng. A 745 (2019) 411–419.
[15] J.H. Zhang, S.J. Liu, R.Z. Wu, L.G. Hou, M.L. Zhang, J. Magn. Alloy 6 (2018) 277–291.
[16] I.H. Jung, M. Sanjari, J. Kim, S. Yue, Scr. Mater. 102 (2015) 1–6.
[17] M. Yamasaki, T. Anan, S. Yoshimoto, Y. Kawamura, Scr. Mater. 53 (2005) 799–803.
[18] B.J. Wang, D.K. Xu, S.D. Wang, L.Y. Sheng, R.C. Zeng, E.H. Han, Int. J. Fatigue 120 (2019) 46–55.
[19] R. Arrabal, E. Matykina, A. Pardo, M.C. Merino, K. Paucar, M. Mohedano, P. Casajús, Corros. Sci. 55 (2012) 351–362.
[20] R.G. Li, D.Y. Zhao, J.H. Zhang, H.R. Li, Y.Q. Dai, D.Q. Fang, Mater. Sci. Eng. A 787 (2020) 139551.
[21] X.B. Zhang, Z.X. Ba, Z.Z. Wang, Y.J. Xue, Corros. Sci. 105 (2016) 68–77.
[22] M. Esmaily, J.E. Svensson, S. Fajardo, N. Birbilis, G.S. Frankel, S. Virtanen, R. Arrabal, S. Thomas, L.G. Johansson, Prog. Mater. Sci. 89 (2017) 92–193.
[23] L. Yang, Y. Huang, F. Feyerabend, R. Willumeit, C. Mendis, K.U. Kainer, N. Hort, Acta Biomater. 9 (2013) 8499–8508.
[24] X.R. Chen, S.C. Ning, A. Wang, Q.C. Le, Q.Y. Liao, Y.H. Jia, C.L. Cheng, X.Q. Li, A. Atrens, F.X. Yu, Corros. Sci. 163 (2020) 108289.
[25] J.H. Zhang, D.X. Tang, H.J. Zhang, L.M. Wang, J. Wang, J. Meng, Chin. J. Rare Met. 32 (2008) 659–667.
[26] Z.J. Wang, Y.H. Huang, Y. Yang, J.C. Wang, C.T. Liu, Scr. Mater. 94 (2015) 28–31.
[27] A.Y. Joseph, G.H.J. Louis, R.T. Dallas, Acta Mater. 58 (2010) 5704–5713.
[28] N. Mo, I.M. Carroll, Q.Y. Tan, A. Ceguerra, Y. Liu, J.L. Cairney, H. Dieringa, Y.D. Huang, B. Jiang, F.S. Pan, M. Berminghama, M.X. Zhang, Acta Mater. 181 (2019) 185–199.
[29] C.X. Xu, B.F. Lu, Z.L. Lv, W. Liang, J. Rare Earth 26 (2008) 604–608.
[30] M.Q. Zhang, Y. Feng, J.H. Zhang, S.J. Liu, Q. Yang, Z. Liu, R.G. Li, J. Meng, R.Z. Wu, J. Mater. Sci. Technol. 35 (2019) 2365–2374.
[31] G.D. Tong, H.F. Liu, Y.H. Liu, Trans. Nonferrous Met. Soc. China 20 (2010) s336–s340.
[32] Y.X. Wang, J.W. Fu, Y.S. Yang, Trans. Nonferrous Met. Soc. China 22 (2012) 1322–1328.
[33] J. Zhang, Q. Ma, F.S. Pan, Mater. Sci. Forum 654-656 (2010) 643–646.
[34] H. Lin, M.B. Yang, H. Tang, F.S. Pan, Prog. Nat. Sci. 28 (2018) 66–73.
[35] F. Zhong, H.J. Wu, Y.L. Jiao, R.Z. Wu, J.H. Zhang, L.G. Hou, M.L. Zhang, J. Mater. Sci. Technol. 39 (2020) 124–134.
[36] C. You, C.M. Liu, Y.C. Wan, B. Tang, B.Z. Wang, Y.H. Gao, X.Z. Han, J. Magn. Alloy 7 (2019) 414–418.
[37] J.F. Nie, Metall. Mater. Trans A 43 (2012) 3891–3939.
[38] H. Liu, W.F. Xu, N.C. Wilson, L.M. Peng, J.F. Nie, J. Alloy Compd. 712 (2017) 334–344.
[39] Y. Zhang, W. Rong, Y.J. Wu, L.M. Peng, J.F. Nie, N. Birbilis, J. Alloy Compd. 777 (2019) 531–543.
[40] J. Tan, Y. Dong, H.X. Zhang, Y.H. Sun, B.Z. Sun, Y. Qi, Scr. Mater. 172 (2019) 130–134.
[41] K. Saito, H. Kaneki, J. Alloy Compd. 574 (2013) 283–289.
[42] H.B. Xie, B.S. Liu, J.Y. Bai, C.L. Guan, D.F. Lou, X.Y. Pang, H. Zhao, S.S. Li, Y.P. Ren, H.C. Pan, C.L. Yang, G.W. Qin, J. Alloy Compd. 814 (2020) 152320.
[43] Y.M. Zhu, K. Ohishi, N.C. Wilson, K. Hono, A.J. Morton, J.F. Nie, Metall. Mater. Trans A 47A (2015) 927–940.
[44] J.F. Nie, K. Oh-ishi, X. Gao, K. Hono, Acta Mater. 56 (2008) 6061–6076.
[45] J.K. Zheng, C.Y. Zhu, Z. Li, R.C. Luo, X.Q. Zeng, B. Chen, Mater. Lett. 238 (2019) 66–69.
[46] W. Rong, Y.J. Wu, Y. Zhang, M. Sun, J. Chen, L.M. Peng, W.J. Ding, Mater. Charact. 126 (2017) 1–9.
[47] J.H. Zhang, M.L. Zhang, J. Meng, R.Z. Wu, D.X. Tang, Mat. Sci. Eng. A 527 (2010) 2527–2537.
[48] F.Z. Meng, S.H. Lv, Q. Yang, P.F. Qin, J.H. Zhang, K. Guan, Y.D. Huang, N. Hort, B.S. Li, X.J. Liu, J. Meng, J. Alloy Compd. 795 (2019) 436–445.
[49] K. Guan, F.Z. Meng, P.F. Qin, Q. Yang, D.D. Zhang, B.S. Li, W. Sun, S.H. Lv, Y.D. Huang, N. Horte, J. Meng, J. Mater. Sci. Technol. 35 (2019) 1368–1377.
[50] G.L. Song, B. Johannesson, S. Hapugoda, D. StJohn, Corros. Sci. 46 (2004) 955–977.
[51] N. Pebere, C. Riera, F. Dabosi, Electrochim. Acta 35 (1990) 555–561.
[52] G.L. Song, A. Atrens, D. Stjohn, J. Nairn, Y. Li, Corros. Sci. 39 (1997) 855–875.
[53] G.L. Makar, J. Kruger, Int. Mater. Rev. 38 (1993) 138–153.
[54] G.L. Song, A. Atrens, Adv. Eng. Mater. 1 (1999) 11–33.
[55] G.L. Song, Adv. Eng. Mater. 7 (2005) 563–586.
[56] R. Pinto, M.G.S. Ferreira, M.J. Carmezim, M.F. Montemor, Electrochim. Acta 56 (2011) 1535–1545.
[57] G.L. Song, D.Y. Shan, E.H. Han, J. Mater. Sci. Technol. 33 (2017) 954–960.
[58] J.H. Liu, Y.W. Song, J.C. Chen, P. Chen, D.Y. Shan, E.H. Han, Electrochim. Acta 189 (2016) 190–195.
[59] W.E. Mercer, J.E. Hill, SAE Technical Paper, 1992.
[60] X.H. Zhou, Y.W. Huang, Z.L. Wei, Q.R. Chen, F.X. Gan, Corros. Sci. 48 (2006) 4223–4233.
[61] K.D. Ralston, N. Birbilis, C.H.J. Davies, Scr. Mater. 63 (2010) 1201–1204.
[62] T.X. Zheng, Y.B. Hu, S.W. Yang, J. Magn. Alloy 5 (2017) 404–411.
[63] R.C. Zeng, K.U. Kainer, C. Blawert, et al., J. Alloy Compd. 509 (2011) 4462–4469.

[64] N.N. Aung, W. Zhou, Corros. Sci. 52 (2010) 589–594.
[65] G.R. Argade, S.K. Panigrahi, R.S. Mishra, Corros. Sci. 58 (2012) 145–151.
[66] M. Alvarez-Lopez, M.D. Pereda, J.A.D. Valle, M. Fernandez-Lorenzo, M.C. Garcia-Alonso, O.A. Ruano, Acta Biomater. 6 (2010) 1763–1771.
[67] Y.L. Song, Y.H. Liu, S.R. Yu, et al., J. Mater. Sci. 42 (2007) 4435–4440.
[68] Y. Jie, D.Q. Yi, S.H. Deng, B. Wang, G.Q. Liu, J. Chin. Soc. Corros. Prot. 28 (2008) 205–209.
[69] G.L. Song, A. Atrens, X. Wu, et al., Corros. Sci. 40 (1998) 1769–1791.
[70] G.L. Song, Corros. Prevent. Magn. Alloys (2013) 3–37, doi:10.1533/9780857098962.1.3.
[71] G.L. Song, A. Atrens, M. Dargusch, Corros. Sci. 41 (1999) 249–273.
[72] G.L. Song, D. Stjohn, J. Light Met. 2 (2002) 1–16.
[73] S.Q. Yin, W.C. Duan, W.H. Liu, L. Wu, J.M. Yu, Z.L. Zhao, M. Liu, P. Wang, J.Z. Cui, Z.Q. Zhang, Corros. Sci. 166 (2020) 108419.
[74] W.J. Liu, F.H. Cao, L.R. Chang, Z. Zhang, J.Q. Zhang, Corros. Sci. 51 (2009) 1334–1343.
[75] W.J. Liu, F.H. Cao, A. Chen, L.R. Chang, J.Q. Zhang, C.N. Cao, Corros. Sci. 52 (2010) 627–638.
[76] J.W. Chang, X.W. Guo, S.M. He, P.H. Fu, L.M. Peng, W.J. Ding, Corros. Sci. 50 (2008) 166–177.
[77] T. Takenaka, T. Ono, Y. Narazaki, Y. Naka, M. Kawakami, Electrochim. Acta 53 (2007) 117–121.
[78] F. Rosalbino, E. Angelini, S. De Negri, A. Saccone, S. Delfino, Intermetallics 14 (2006) 1487–1492.
[79] J.H. Liu, E.H. Han, Y.W. Song, D.Y. Shan, J. Alloy Compd. 757 (2018) 356–363.
[80] O.I. Velikokhatnyi, P.N. Kumta, Acta Biomater. 6 (2010) 1698–1704.
[81] J.Y. Zhang, M. Xu, X.Y. Teng, M. Zuo, J. Magn. Alloy 4 (2016) 319–325.
[82] R.C. Zeng, L. Sun, Y.F. Zheng, et al., Corros. Sci. 79 (2014) 69–82.
[83] N.Y. Li, R. Osborne, B. Cox, D. Penrod, SAE Technical Paper Series, 2005, doi:10.4271/2005-01-0337.
[84] J. Aragones, K. Goundan, S. Kolp, R. Osborne, L. Ouimet, W. Pinch, SAE Technical Paper Series, 2005, doi:10.4271/2005-01-0340.
[85] S. Koike, K. Washizu, S. Tanaka, T. Baba, K. Kikawa, SAE Technical Paper Series, 2000, doi:10.4271/2000-01-1117.
[86] J. Yang, J. Wang, W.L. Xiao, L.D. Wang, Y.M. Wu, H.J. Zhang, L.M. Wang, Mater. Sci. Forum 561-565 (2007) 199–202.
[87] L. Yang, Y. Huang, Q. Peng, F. Feyerabend, K.U. Kainer, R. Willumeit, et al., Mater. Sci. Eng. B 176 (2011) 1827–1834.
[88] L. Yang, Y. Huang, F. Feyerabend, R. Willumeit, K.U. Kainer, N. Hort, J. Mech. Behav. Biomed. Mater. 13 (2012) 36–44.
[89] N. Hort, Y. Huang, D. Fechner, M. Störmer, C. Blawert, F. Witte, C. Vogt, H. Drücker, R. Willumeit, K.U. Kainer, F. Feyerabend, Acta Biomater. 6 (2010) 1714–1725.
[90] Q.T. Jiang, X.Z. Lv, D.Z. Lu, J. Zhang, B.R. Hou, J. Magn. Alloy 6 (2018) 346–355.
[91] A.D. Sudholz, K. Gusieva, X.B. Chen, et al., Corros. Sci. 53 (2011) 2277–2282.
[92] D.K. Xu, W.N. Tang, L. Liu, Y.B. Xu, E.H. Han, J. Alloy Compd. 432 (2007) 129–134.
[93] S.Q. Yin, Z.Q. Zhang, X. Liu, Q.C. Le, Q. Lan, L. Bao, J.Z. Cui, Mater. Sci. Eng. A 695 (2017) 135–143.
[94] A. Niikura, A.P. Tsai, Phil. Mag. Lett. 69 (1994) 351–355.
[95] A. Singh, M. Watanabe, A. Kato, A.P. Tsai, Acta Mater. 53 (2005) 4733–4742.
[96] A. Singh, Sci. Technol. Adv. Mater. 15 (2014) 044803.
[97] A. Singh, A.P. Tsai, Scr. Mater. 53 (2005) 1083–1087.
[98] J. Wang, S. Gao, P. Song, X. Huang, Z. Shi, F. Pan, J. Alloy Compd. 509 (2011) 8567–8572.
[99] A. Singh, M. Nakamura, M. Watanabe, A. Kato, A.P. Tsai, Scr. Mater. 49 (2003) 417–422.
[100] E.L. Zhang, W.W. He, H. Du, K. Yang, Mater. Sci. Eng. A 488 (2008) 102–111.
[101] D.Q. Wan, G.C. Yang, M. Zhu, Acta Metall. Sin. 20 (2007) 429–433.
[102] D.A. Basha, J.M. Rosalie, H. Somekawa, T. Miyawaki, A. Singh, K. Tsuchiya, Sci. Technol. Adv. Mat. 17 (2016) 115–127.
[103] Y.W. Song, D.Y. Shan, R.S. Chen, E.H. Han, Corros. Sci. 52 (2010) 1830–1837.
[104] A. Srinivasan, Y. Huang, C.L. Mendis, C. Blawert, K.U. Kainer, N. Hort, Mater. Sci. Eng. A 595 (2014) 224–234.
[105] R.H. Buzolin, M. Mohedano, C.L. Mendis, B. Mingo, D. Tolnai, C. Blawert, K.U. Kainer, H. Pinto, N. Hort, Mater. Sci. Eng. A 682 (2017) 238–247.
[106] Y. Kawamura, K. Hayashi, A. Inoue, T. Masumoto, Mater. Trans. 7 (2001) 1172–1176.
[107] E. Abe, Y. Kawamura, K. Hayashi, A. Inoue, Acta Mater. 50 (2002) 3845–3857.
[108] Y.M. Zhu, A.J. Morton, J.F. Nie, Acta Mater. 58 (2010) 2936–2947.
[109] J.F. Nie, Y.M. Zhu, A.J. Morton, Metall. Mater. Trans. A 194 (2014) 3338–3348.
[110] Y.M. Zhu, A.J. Morton, J.F. Nie, Acta Mater. 60 (2012) 6562–6572.
[111] M. Matsuda, S. Li, Y. Kawamura, Y. Ikuhara, M. Nishida, Mater. Sci. Eng. A 393 (2005) 269–274.
[112] D. Egusa, E. Abe, Acta Mater. 60 (2012) 166–178.
[113] C.Q. Li, D.K. Xu, Z.R. Zeng, B.J. Wang, L.Y. Sheng, X.B. Chen, E.H. Han, Mater. Des. 121 (2017) 430–441.
[114] Z.Q. Zhang, X. Liu, W.Y. Hu, J.H. Li, Q.C. Le, L. Bao, Z.J. Zhu, J.Z. Cui, J. Alloy Compd. 624 (2015) 116–125.
[115] Z. Leng, J.H. Zhang, T.T. Yin, L. Zhang, X.Y. Guo, Q.M. Peng, M.L. Zhang, R.Z. Wu, J. Mech. Behav. Biomed. 28 (2013) 332–339.
[116] Q.M. Peng, J.X. Guo, H. Fu, X.C. Cai, Y.N. Wang, B.Z. Liu, Z.G. Xu, Sci. Rep. 4 (2014) 3620.
[117] L.S. Wang, J.H. Jiang, T. Yuan, Q.Y. Xie, H. Liu, A.B. Ma, Met. Mater. Int. (2019), doi:10.1007/s12540-019-00410-3.
[118] X.H. Shao, Z.Z. Peng, Q.Q. Jin, X.L. Ma, Acta Mater. 118 (2016) 177–186.
[119] X.H. Shao, Z.Q. Yang, X.L. Ma, Acta Mater. 58 (2010) 4760–4771.
[120] M. Yamasaki, M. Sasaki, M. Nishijima, K. Hiraga, Y. Kawamura, Acta Mater. 55 (2007) 6798–6805.
[121] C. Xu, T. Nakata, X. Qiao, M. Zheng, K. Wu, S. Kamado, Sci. Rep. 7 (2017) 40846.
[122] J.H. Zhang, C. Xu, Y.B. Jing, S.H. Lv, S.J. Liu, D.Q. Fang, J.P. Zhuang, M.L. Zhang, R.Z. Wu, Sci. Rep. 5 (2015) 13933.
[123] Y.F. Jiao, J.H. Zhang, P.Y. Kong, Z.W. Zhang, Y.B. Jing, J.P. Zhuang, W. Wang, L. Zhang, C. Xu, R.Z. Wu, M.L. Zhang, J. Mater. Chem. B 3 (2015) 7386–7400.
[124] L. Zhang, J.H. Zhang, C. Xu, Y.B. Jing, J.P. Zhuang, R.Z. Wu, M.L. Zhang, Mater. Lett. 133 (2014) 158–162.
[125] W.W. Jian, G.M. Cheng, W.Z. Xu, H. Yuan, M.H. Tsai, Q.D. Wang, C.C. Koch, Y.T. Zhu, S.N. Mathaudhu, Mater. Res. Lett. 1 (2013) 61–66.
[126] P. Bakke, H. Westengen, K. Pettersen, SAE Technical Paper Series, 2003, doi:10.4271/2003-01-0189.
[127] P. Bakke, H. Westengen, Adv. Eng. Mater. 5 (2003) 879–885.
[128] J.H. Zhang, D.P. Zhang, Z. Tian, J. Wang, K. Liu, H.Y. Lu, D.X. Tang, J. Meng, Mat. Sci. Eng. A 489 (2008) 113–119.
[129] J.H. Zhang, Z. Leng, M.L. Zhang, J. Meng, R.Z. Wu, J. Alloy Compd. 509 (2011) 1069–1078.
[130] J.H. Zhang, J. Wang, X. Qiu, D.P. Zhang, Z. Tian, X.D. Niu, D.X. Tang, J. Meng, J. Alloy Compd. 464 (2008) 556–564.
[131] J.H. Zhang, K. Liu, D.Q. Fang, X. Qiu, P. Yu, D.X. Tang, J. Meng, J. Alloy Compd. 480 (2009) 810–819.
[132] J.X. Niu, Q.R. Chen, N.X. Xu, Z.L. Wei, Trans. Nonferrous Met. Soc. China 18 (2008) 1058–1064.
[133] J.H. Zhang, X.D. Niu, X. Qiu, K. Liu, C.M. Nan, D.X. Tang, J. Meng, J. Alloy Compd. 471 (2009) 322–330.
[134] P. Cheng, Y.H. Zhao, R.P. Lu, H. Hou, J. Alloy Compd. 764 (2018) 226–238.
[135] G.L. Bi, Y.D. Li, S.J. Zang, J.B. Zhang, Y. Ma, Y. Hao, J. Magn. Alloy 2 (2014) 64–71.
[136] A. Boby, A. Srinivasan, U.T.S. Pillai, B.C. Pai, Mater. Des. 88 (2015) 871–879.